Proposal for a rotation-sensing interferometer with spin-orbit-coupled atoms

Yan-Xiong Du, Hui Yan, Dan-Wei Zhang, Chuan-Jia Shan, and Shi-Liang Zhu

Proposal to realize a rotation sensing interferometer with spin-orbit coupled atoms

Yan-Xiong Du,[1] Hui Yan,[1, *] Dan-Wei Zhang,[1] Chuan-Jia Shan,[1] and Shi-Liang Zhu[1, 2, †]

[1]*Laboratory of Quantum Information Technology,*
School of Physics and Telecommunication Engineering,
South China Normal University, Guangzhou 510006, China
[2]*Center for Quantum Information, IIIS, Tsinghua University, Beijing, China*

We propose a theoretical scheme to realize a rotation sensing interferometer with spin-orbit coupled atoms. The sensitivity of this kind interferometer is dependent of the atomic mass $m^{-\alpha}$ with a factor $\alpha \geq 1$. Thus the sensitivity can be improved by about one order of magnitude when we choose Li instead of Rb. Furthermore, comparing to the standard Raman interferometer, the response to high-frequency time-dependent rotation can be improved through the continuous coupling between spin and orbital freedoms of the atoms.

I. INTRODUCTION

Matter-wave interferometry has been proved to be a powerful tool for precision metrology [1–4]. For example, neutron and atomic interferometers have been used to measure the rotation of the Earth and the acceleration due to the gravity [5–8]. Other experiments described in Refs. [9–11] give accurate results of measuring the surface gravity and various fundamental constants. Up to now, many kinds of methods can be used to coherently split the atoms, such as transmission grating [12], double slits [13] and standing light wave [14]. Currently, with the rapid developing of the neutral atom cooling and trapping techniques, Raman or Brag pulses have been used to manipulate the spin states [3, 15, 16], where recent excited progress is achieved with momentum splitting up to 102 photon recoil momentum [17].

The phase shift of a matter-wave Sagnac interferometer can be described by $\phi_{\text{Sagnac}} = \frac{4\pi m}{h} \boldsymbol{S} \cdot \boldsymbol{\omega}$[18], where $\boldsymbol{\omega}$ is the angular velocity of rotation, $\boldsymbol{S}$ is the enclosing area, and h is the Planck constant. Since the atomic mass m is much larger than the photon mass $\frac{h\nu}{c^2}$, the sensitivity of the matter-wave Sagnac interferometer is much larger than the photon ones. However, as for the Raman or Brag atomic interferometer, one should find that the phase shift $\phi_{Sagnac} = 2k_r v T^2 \omega$ is actually independent of m, since the enclosing area is $S = \hbar k_r v T^2 / m$, where v is the velocity of atoms, k_r represents the recoil momentum and T is the drifting time. Therefore, people always are struggling to increase T [19] and k_r to improve the sensitivity[17, 20, 21]. However, the increasing of operating time is always along with the dropping of cutoff frequency.

In this paper, we propose a theoretical scheme to realize a rotation sensing interferometer with spin-orbit (SO) coupled atoms, where the SO coupling is induced by a synthetic gauge field. The synthetic gauge field has emerged as a tool for quantum simulation recently, such as quantum Hall effects [22–24], Bose-Hubbard model [25–27], Majorana fermions [28] and topological insulators[29]. It is notable that a typical SO coupling for cold atoms has been realized experimentally[30, 31]. For such an interferometer, the phase shift is dependent of the atomic mass. Thus the sensitivity can be improved by at least one order of magnitude with the same operating time when we choose Li instead of Rb, compared with the Raman atomic interferometer. Another important characteristic of this SO coupling atomic interferometer is that, it is more sensitive to high-frequency time-dependent rotation and thus has higher cutoff frequency[32].

The paper is organized as follows: Section II introduces the dressed states and the manipulation, such as the $\pi/2$ and π pulses in the dressed state representation which are useful in the atomic interferometers. Section III shows how to construct the rotation sensing atomic interferometers with SO coupled atoms. In Sec. IV we discuss the measurement characteristics of the interferometers. A brief discussion and short conclusion are given in Sec. V.

II. DRESSED STATES AND THE MANIPULATION

For the Raman-type interferometer, the interference is based on coherently manipulating the atomic internal states. Here, we would like to introduce the dressed state atomic interferometer, where the interference is based on the manipulation of the atomic dressed states in parameter space or in real space. We consider a diluted cold atomic gas in a harmonic trap, where each atom has a three-level Λ-type configuration, as shown in Fig. 1(a). Two counter-propagating laser beams with the corresponding Rabi frequencies Ω_1 and Ω_2 are used to couple the ground states $|1\rangle$ and $|2\rangle$ to the excited state $|3\rangle$, with the same large detuning Δ. In the interaction picture, the laser-atom interaction Hamiltonian H_0 is given
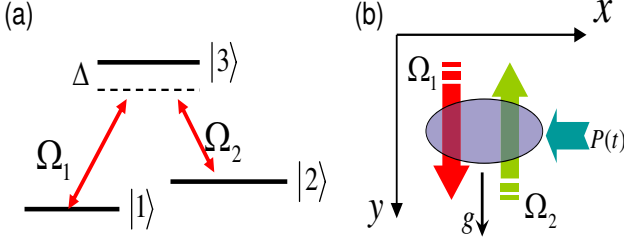
FIG. 1: (color online). (a) Three-level Λ atomic system coupled with two laser beams characterized by the Rabi frequencies Ω_1 and Ω_2 with a large single-photon detuning Δ. (b) Schematic representation of laser-atom interaction. The Rabi frequencies Ω_1, Ω_2 are space-dependent and will exist along the whole process, while $P(t)$ are the $\pi/2 - \pi - \pi/2$ sequences in the dressed states.

by

$$H_0 = -\hbar(\Omega_1|1\rangle\langle3| + \Omega_2|2\rangle\langle3| + 2\Delta|3\rangle\langle3|) + \text{H.c.,} \quad (1)$$

where the Rabi frequencies $\Omega_1 = \Omega\sin\theta e^{i\varphi}$ and $\Omega_2 = \Omega\cos\theta$ with $\Omega = \sqrt{|\Omega_1|^2 + |\Omega_2|^2}$ (θ, φ are the variable parameters). Under the dressed state representation, we get a unitary matrix Γ related the dressed states $|\chi\rangle = (|\chi_1\rangle, |\chi_2\rangle, |\chi_3\rangle)^{Tr}$ to the bare states $(|1\rangle, |2\rangle, |3\rangle)^{Tr}$ (Tr denotes the transposition), while the dressed states $|\chi\rangle$ are the eigenstates of the Hamiltonian (1) with the corresponding eigenvalues $\lambda = (0, \Delta - \sqrt{\Delta^2 + \Omega^2}, \Delta + \sqrt{\Delta^2 + \Omega^2})$. The matrix Γ is given by

$$\Gamma = \begin{pmatrix} \cos\theta & -\sin\theta e^{-i\varphi} & 0 \\ \sin\theta\cos\gamma e^{i\varphi} & \cos\theta\cos\gamma & -\sin\gamma \\ \sin\theta\sin\gamma e^{i\varphi} & \cos\theta\sin\gamma & \cos\gamma \end{pmatrix}, \quad (2)$$

where γ is determined by $\tan\gamma = (\sqrt{\Delta^2 + \Omega^2} - \Delta)/\Omega$ [23]. Using the large detuning condition $\Delta \gg \Omega$, we could get $\gamma \to 0$ since $\tan\gamma$ tends to zero. Then the two lower dressed states $\{|\chi_1\rangle, |\chi_2\rangle\}$ have negligible contribution from the excited state $|3\rangle$. Thus a subspace is spanned by the two lower dressed states $\{|\chi_1\rangle, |\chi_2\rangle\}$, where

$$\begin{aligned} |\chi_1\rangle &= \cos\theta|1\rangle - \sin\theta e^{-i\varphi}|2\rangle, \\ |\chi_2\rangle &= \sin\theta e^{i\varphi}|1\rangle + \cos\theta|2\rangle. \end{aligned} \quad (3)$$

We may use other two similar laser beams to realize π and $\pi/2$ pulses in the dressed-state-space which are required for the atom interferometer (see the next section). The β $(= \pi, \pi/2)$ pulse is defined as $U_p = e^{-i\beta\sigma_y'/2}$, where $\sigma_y' \equiv i(|\chi_2\rangle\langle\chi_1| - |\chi_1\rangle\langle\chi_2|)$ is the Pauli matrix applying on the dressed-state-space $\{|\chi_1\rangle, |\chi_2\rangle\}$. Since the phase in Eq.(3) is actually irrelevant to the sensitivity of the atomic interferometer, we may simply choose it to be zero (i.e., let the two lasers represented by Ω_1 and Ω_2 have the same phases). Under this condition, we have a simple relation $\sigma_y' = \sigma_y$, where $\sigma_y \equiv i(|2\rangle\langle1| - |1\rangle\langle2|)$ is the Pauli matrix applying on space $\{|1\rangle, |2\rangle\}$. We may use this relation to realize the required β pulse.

For concreteness, we choose the Rabi frequencies co-propagating along the x axis to be $\Omega_{p1} = \Omega_{p2}e^{i\pi/2}$, see $P(t)$ in Fig.1(b). The corresponding Hamiltonian H_p in the bare energy basis $\{|1\rangle, |2\rangle, |3\rangle\}$ is then written as

$$H_p = \hbar \begin{pmatrix} 0 & 0 & \Omega_{p1} \\ 0 & 0 & \Omega_{p2} \\ \Omega_{p1}^* & \Omega_{p2}^* & 2\Delta \end{pmatrix}. \quad (4)$$

It is straightforward to show that the effective Hamiltonian projected to the subspace $\{|1\rangle, |2\rangle\}$ under the large detuning case (i.e., $\Delta \gg |\Omega_{p1}|, \Omega_{p1}|$) is given by $H_p' = \hbar\delta(1 + \sigma_y)$ with $\delta = \frac{|\Omega_{p1}^*\Omega_{p2}|}{2\Delta}$. Since $\sigma_y' = \sigma_y$ in the case $\varphi = 0$, we derive an evolution operator $U_p = e^{-i\beta\sigma_y'/2}$ with $\beta = 2\delta t_p$ up to an irrelevant overall phase $e^{-i\delta t_p}$ when the applying time of the pulse $P(t)$ is t_p. Therefore, we can realize the operators $\pi/2 - \pi - \pi/2$ sequences between the dressed states $|\chi_1\rangle$ and $|\chi_2\rangle$, which are required by the dressed state interferometer, by turning on two pulse lasers for suitable time t_p.

III. ROTATION SENSING DRESSED STATE ATOMIC INTERFEROMETER

After the first $\pi/2$ pulse, the harmonic trap is turned off at time $t = 0$, and the atoms fall off due to gravity with an acceleration $g = 9.8 m/s^2$ (along the direction $\mathbf{e}_y$). In the whole process the above configuration of the light-atom coupling exists and leads to a gauge field. Different dressed states will experience different spatially varying gauge field in this space-varying laser fields, which can be used to realize the splitting and recombination of the atoms for an area enclosing interferometer. This idea is different with the Raman-type interferometer [15] where the Raman pulses change the internal states as well as the external states. As shown in Fig.1(b), we consider in this paper that two counterpropagating Gaussian laser beams are given by $\Omega_j(x) = \Omega_0 exp[-(x - x_j)^2/\sigma_0^2]exp(-ik_jy)$, $(j = 1, 2)$ [23], where the propagating wave vectors $k_1 = -k_2 = k/2$ and the center position $x_1 = -x_2 = \Delta x/2$. Then the effective Hamiltonian reads

$$H_\sigma = \frac{1}{2m}(-i\hbar\nabla - \boldsymbol{A}_\sigma)^2 + V_\sigma(\boldsymbol{r}), \quad (5)$$

where $\sigma = \pm 1$ represent the pseudo spin $|\chi_1\rangle$ and $|\chi_2\rangle$, respectively. The gauge potential in real space is given by $\boldsymbol{A}_\sigma = \frac{\sigma\hbar k}{1+exp(-x/d)}\boldsymbol{e}_y$ with $d = \sigma_0^2/(4\Delta x)$. The Hamiltonian (5) is actually equivalent to that of a particle with SO coupling $\sigma_z p_y$ [23]. The scalar potential V_σ has small modification toward the motion of atom. The synthetic magnetic field has the form

$$\boldsymbol{B}_\sigma = \frac{\sigma\hbar k}{4d\cosh^2(x/2d)}\boldsymbol{e}_z, \quad (6)$$

and its spatial distribution is illustrated in Fig.2(a) for the typical parameters $\Delta x_0 = 2.5\mu m$, $\sigma_0 = 10\mu m$ and
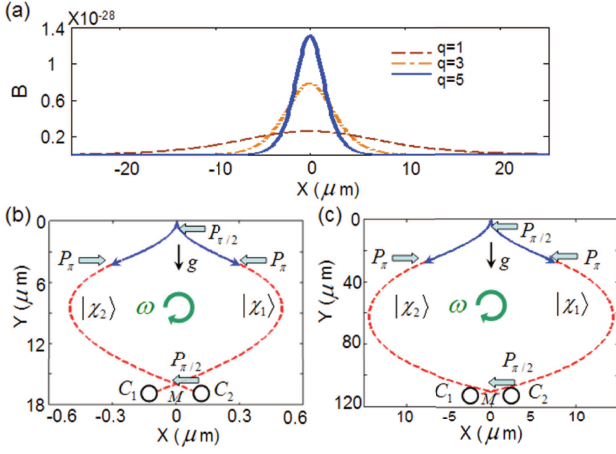
FIG. 2: (color online). (a) The distribution of synthetic magnetic field along x axis with different parameter q. (b-c) Spin-dependent trajectories of a single Rb atom in (b) and atom Li in (c) during the procession in the rotating frame ω. The division of superposition state induced by the space-dependent Rabi frequencies is illustrated by the blue solid lines. We recombine the atom by a π pulse and then the atom is traveling along the red dashed lines and interfere at point M. The atoms collected by the collectors C_1, C_2 will be used to examine the interference induced by rotation ω. The other parameters $\Delta x_0 = 2.5\mu$m, $\sigma_0 = 10\mu$m and $k = 10^7$ m^{-1}.

$k = 10^7$ m^{-1}. There is a peak at $x = 0$. Increasing the separation $q = \Delta x/\Delta x_0$ between the lasers will improve the maximal value of B_σ, while the spatial distribution will shrink, since the total effect is limited by the photon recoil momentum through the relation $\int B dx = 2\hbar k_r$.

The trajectories of atoms are determined by the Heisenberg equations of motion with the initial condition $\boldsymbol{r} = \boldsymbol{0}$, $\dot{\boldsymbol{r}} = \boldsymbol{0}$. Therefore, after switching off the harmonic trap at $t = 0$, the atoms will fall off due to the gravity, and split into two parts in the gauge field. After the π pulse, the atoms will recombine and enclose an area as illustrated in Fig.2(b) for the atom Rb. As for a typical example shown in Fig. 2(b), the π pulse is applying at $t_d = 0.19$ms to reverse the pseudo spin states. Then the dressed states will feel an opposite force in the synthetic field, as shown by the red dashed lines in Fig.2(b). The two arms will meet at point M after $t_c = 0.683$ms, t_c is the time that the final $\pi/2$ pulse is applying. As shown in Fig.3, t_c increases linearly with t_d for t_d less than 1 ms and then ramps quickly after that. The atoms from two arms will interfere after eliminating the path information by another $\pi/2$ pulse. In the operator language such pulse sequences are described as

$$U_s = P_{\pi/2}(t_c + t_d)S(B^-)P_\pi(t_d)S(B^+)P_{\pi/2}(0), \quad (7)$$

where $S(B^+)$, $S(B^-)$ stand for the interaction of synthetic magnetic field along the trajectories. For comparison, the trajectories of Li atom are plotted in Fig. 2(c) for the same parameters except of the atomic mass. It is
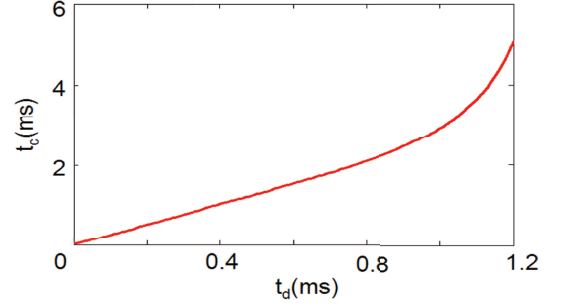

FIG. 3: (color online). The relationship between the division time t_d and the recombination time t_c.

shown that the enclosed area of Li is much larger than that of Rb.

The phase difference $\Delta\phi$ contains the following three typical contributions

$$\Delta\phi = \phi_{\text{Sagnac}} + \phi_{grav} + \phi_{LA}, \quad (8)$$

where ϕ_{Sagnac} is the usual Sagnac phase difference due to rotation. ϕ_{grav} represents the contribution from gravity. It is clear that the two interfering arms accumulate equal phases and therefore $\phi_{grav} = 0$ as a result of the reflection symmetry of the system. In addition, the emergence of gravity breaks the time-reversal symmetry of the quantum system, making the interfering arms stretch along the direction of gravity as time passes. The last term ϕ_{LA} origins from the interaction between lasers and atoms since the lasers may bring in an external phase difference in general. The system can be viewed as a charged particle with the charge $\sigma = \pm 1$ moving in an effective magnetic field $\boldsymbol{B}_\sigma$ and thus the wave function picks up a phase factor $\exp(\frac{-i\sigma}{\hbar c}\int \boldsymbol{A}d\boldsymbol{l})$. Because of the $\pi/2$ pulses, the atom goes through the two trajectories at the same time and senses the opposite field. As a result, the total magnetic flux is zero which implies no external optical phase. Therefore, the interference is determined just by the Sagnac phase shift.

The final detection of interference is determined by the pseudo-spin population difference, which can be examined by the atomic population of state $|\chi_1\rangle$ in the collectors C_1, C_2, i.e.,

$$N_1 = \frac{N}{2}(1 + \cos\Delta\phi), N_2 = \frac{N}{2}(1 - \cos\Delta\phi). \quad (9)$$

Here N is the total atomic number. N_1, N_2 are the atomic populations of dressed state $|\chi_1\rangle$ collected by C_1, C_2, respectively. Usually, to make sure that purely the population in state $|\chi_1\rangle$ is detected, one can transfer the state $|\chi_2\rangle$ to a different hyperfine ground state $|H\rangle$ by another Rabi frequency that couples state $|3\rangle$ with state $|H\rangle$ [23].
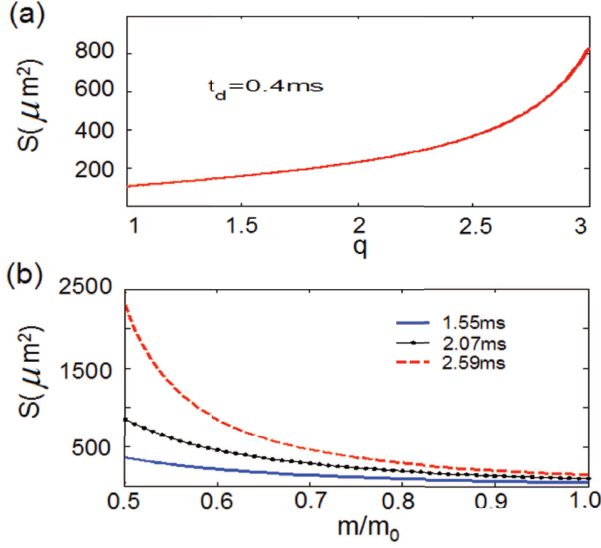
FIG. 4: (color online). (a) The enclosing area S versus parameter q with the division time $t_d = 0.4ms$. (b) Area S verses the ratio m/m_0 with different max operating time.

FIG. 5: (color online). (a) Enclosing area in Raman-type interferometers (blue solid line) and in the SO coupling with $q = 1.11$ (red dotted line), $q = 1.43$ (black dashed line) and $t_d = 0.2ms$. As can be seen that the interferometry using gauge field will dominate at lighter mass elements such as Lithium and Sodium. (b) The response factors towards sinusoidal time-varying signal for Raman and SO-type interferometers.

IV. MEASUREMENT CHARACTERISTIC OF THE INTERFEROMETER

Now we are in a position to discuss the measurement characteristics of such a system. The sensitivity of the atomic interferometry is $\kappa = \frac{4\pi m}{h} S$. As shown in Fig.4(a), the enclosing area S, which is proportional to κ, increases with Δx since the inhomogeneous field B_σ will be compressed as Δx increasing. Such characteristic makes it easy to obtain a large area. In addition, for the standard interferometers, the enclosing area is proportional to m^{-1}, whereas the area of the dressed state interferometer is proportional to $m^{-\alpha}$ (the factor $\alpha \approx 2$ when t_d is small). Fig.4(b) shows the area versus the atomic mass with different maximum operating time T_{max}, here m_0 is taken to be the mass of ^{87}Rb. Comparing with the Raman-type interferometer, with the same operating time (T_{max}) and maximum drifting velocity (gT_{max})[34], the proposed interferometer has larger enclosing area for the lighter mass atoms, as shown in Fig.5(a). The sensitivity of Raman atomic interferometer is almost independent of the mass m. In contrast, the sensitivity of the dressed state interferometer increases linearly with the decrease of $\ln(m/m_0)$. So the sensitivity of the rotation-sensing interferometers can be improved at least 10 times with Lithium instead of Rb. Furthermore, increasing the separation between the lasers will improve the enclosing area as shown by the dashed line in Fig.5(a).

It's useful to compare the dressed state method with the standard Raman transition manipulation technique in detecting time-varying signals. The optical method proposed here provides a continuous spin-orbit coupling, so our system has higher sensitivity to the signals than that of th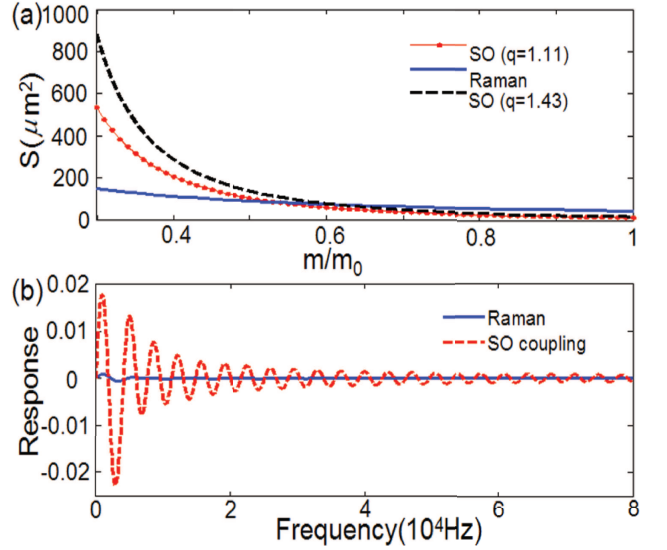e Raman-type, while the latter only couples the spin and orbit in discrete points when laser pulses are shining. An interesting discussion is given in Ref.[32] where the benefits of measuring the gravity signals are demonstrated. In general, a sinusoidal signal $\omega(t) = \omega_z \sin(\omega_0 t)$ with $\omega_z \cdot T_{max} \ll 1$ is applied to the system to investigate the cutoff frequency [15]. In the case of the atoms interacting with the rotating lasers, the Sagnac phase shift is rewritten as

$$\phi_{\text{Sagnac}} = [\frac{m}{\hbar} \int_C \sin(\omega_0 t) \cdot (\boldsymbol{r} \times \boldsymbol{v})_z dt]\omega_z = R\omega_z, \quad (10)$$

where C is the closed path enclosing the area and R is the response factor towards rotation $\omega(t)$. Obvious the response factors R is determined by the velocity and the orbit coupling [35]. We plot the response factors R of the Raman-type and the SO-type in Fig.5(b) in the unit of $mLv/\hbar$, where L is the maximum separation of the interferometers, v is the drifting velocity for Raman type and the average velocity along y for SO coupling system respectively. Since the spin in our system is continuously coupling with the orbit, the final detection of spin states will have much higher response factor than that of the Raman type as shown in Fig.5(b).

V. DISCUSSION AND CONCLUSION

Before concluding, we make some additional comments related to possible concerns in realistic experiments. We

have considered the thermal ensemble of diluted ultra-cold atoms for the convenience of manipulation and detection. So we assume that the atomic gas has a temperature of $1\mu K$ at which it can be well described as a classical gas. Under this temperature the initial number density and the velocity distribution are both described by Gaussian functions characterized by the corresponding spatial variance σ_r and velocity variance σ_v, respectively. With a similar discussion in Ref. [23], we know that the spatial separation of the atomic ensemble won't be covered by the spread of the ensemble. Nevertheless, such spatial and velocity distributions decrease the interference contrast by a factor $e^{-(1/2)\sigma_\phi^2}$ [3], where the rms $\sigma_\phi = \sqrt{(\sigma_r/r_m)^2 + (\sigma_v/v_m)^2}$ with r_m the maximum spatial separation and v_m the maximum velocity. By choosing typical parameters $\sigma_r = 2\mu m$, $\sigma_v = 0.5$cm/s, $r_m = 30$mm and $v_m = gT = 0.63$cm/s, we obtain a typical reduced factor 0.726. On the other hand, the decay of the excited state $|3\rangle$ is the main source of the decoherence. We introduce a complex detuning $\Delta' = \Delta + i\gamma_e$ to describe this decoherence effect, where γ_e is the spontaneous radiation rate of the excited state

$|3\rangle$. The decoherence time of dressed states can be estimated through $T_D = \frac{2\Delta^2}{\Omega^2\gamma_e}$. By choosing the typical parameters $\Omega = 2\pi \times 0.1$MHz, $\Delta \geq 2\pi \times 100$MHz and $\gamma_e = 2$MHz, we have $T_D \sim 1s$, which is longer enough for an interferometer since the operation time is about 1ms.

In conclusion, we have proposed a theoretical scheme to realize a rotation-sensing interferometer with synthetic gauge field. The sensitivity of this SO coupling system is higher for a low-mass atom. Furthermore, the cutoff frequency of the time-dependent rotation is higher than that of the Raman-type interferometer.

[1] Atom Interferometry, edited by P. R. Berman (Academic Press, New York, 1997).

[2] J. F. Clauser, Physica B **151**, 262 (1988).

[3] A. Cronin, J. Schmiedmayer, and D. E. Pritchard, Rev. Mod. Phys. **81**, 1051 (2009).

[4] J. Wang, L. Zhou, R. B. Li, M. Liu and M. S. Zhan, Front. Phys. China **4**, 179(2009).

[5] R. Colella, A. Overhauser, and S. Werner, Phys. Rev. Lett. **34**, 1472 (1975).

[6] S. Werner, J. L. Staudenmann, and R. Colella, Phys. Rev. Lett. **42**, 1103 (1979).

[7] F. Riehle, Th. Kisters, A. Witte, J. Helmcke and Ch. J. Bordé, Phys. Rev. Lett. **67**, 177 (1991).

[8] M. Kasevich and S.Chu, Appl. Phys. B **54**, 321 (1992).

[9] S. Dimopoulos, P. W. Graham, J. M. Hogan, and M. Kasevich, Phys. Rev. Lett. **98**, 111102 (2007).

[10] A. Peters, K. Y. Chung, and S. Chu, Nature (London) **400**, 849 (1999).

[11] J. B. Fixler, G. T. Foster, J. M. McGuirk and M. A. Kasevich, Science **315**, 74 (2007).

[12] D. W. Keith, M. L. Schattenburg, H. I. Smith, and D. E. Prichard, Phys. Rev. Lett. **61**, 1580 (1988). R. Grisenti, W. Schollkopf, J. Toennies, C. Hegerfeldt, and T. Kohler, Phys. Rev. Lett. **83**, 1775 (1999)

[13] O. Carnal and J. Mlynek, Phys. Rev. Lett. **66**, 2689 (1991); F. Shimizu, K. Shimizu, and H. Takuma, Japanese, J. App. Phys. **31**, L436 (1992).

[14] P. J. Martain, B. G. Oldaker, A. H. Miklich, and D. E. Prichard, Phys. Rev. Lett. **60**, 515 (1988).

[15] M. Kasevich and S. Chu, Phys. Rev. Lett. **67**, 181 (1991). T. L. Gustavson, P. Bouyer, and M. A. Kasevich, Phys. Rev. Lett. **78**, 2046 (1997).

[16] B. Benton, M. Krygier, J. Heward, M. Edwards, and C. W. Clark, Phys. Rev. A **84**, 043648 (2011).

[17] S. W. Chiow, T. Kovachy, H. C. Chien, and M. A. Kase-

vich, Phys. Rev. Lett. **107**, 130403 (2011).

[18] L. A. Page, Phys. Rev. Lett. **35**, 543 (1975); J. Anandan, Phys. Rev. D **15**, 1448 (1977); M. Dresden, and C. N. Yang, Phys. Rev. D **20**, 1846(1979).

[19] L. Zhou, Z. Y. Xiong, W. Yang, B. Tang, W. C. Peng, K. Hao, R. B. Li, M. Liu, J. Wang, and M. S. Zhan, Gen. Relativ. Gravit. **43**, 1931(2011).

[20] S. Chiow, S. Herrmann, S. Chu, and H. Mūller, Phys. Rev. Lett. **103**, 050402(2010).

[21] F. Ruschewitz, J. L. Peng, H. Hinderthr, N. Schaffrath, K. Sengstock, and W. Ertmer, Phys. Rev. Lett. **80**, 3173 (1998).

[22] G. Juzeliūnas, J. Ruseckas, P. Ohberg, and M. Fleischhauer, Phys. Rev. A **73**, 025602 (2006).

[23] S. L. Zhu, H. Fu, C. J. Wu, S. C. Zhang, and L. M. Duan, Phys. Rev. Lett. **97**, 240401 (2006).

[24] X. J. Liu, X. Liu, L. C. Kwek, and C. H. Oh, Phys. Rev. Lett. **98**, 026602 (2007).

[25] M. Niemeyer, J. K. Freericks, H. Monien, Phys. Rev. B **60**, 2357 (1999).

[26] K. Sengupta and N. Dupuis, Phys. Rev. A **71**, 033629 (2005).

[27] T. D. Stanescu, B. M. Anderson, and V. Galitski, Phys. Rev. A **78**, 023616 (2008).

[28] C. Zhang, S. Tewari, R. M. Lutchyn, and S. Das Sarma, Phys. Rev. Lett. **101**, 160401 (2008); M. Sato, Y. Takahashi, and S. Fujimoto, *ibid.*, **103**, 020401 (2009); S. L. Zhu, L.-B. Shao, Z. D. Wang, and L.-M. Duan, *ibid.* **106**, 100404 (2011).

[29] L. B. Shao, S. L. Zhu, L. Sheng, D. Y. Xing, and Z. D. Wang, Phys. Rev. Lett. **101**, 246810 (2008); A Bermudez, N Goldman, A Kubasiak, M Lewenstein, M A Martin-Delgado, New J. Phys. **12**, 033041 (2010); L. Mazza, A. Bermudez, N. Goldman, M. Rizzi, M. A. Martin-Delgado, M. Lewenstein, New J. Phys. **14**, 015007 (2012)

[30] Y. J. Lin, G. Jimenez, and I. B. Spielman, Nature (London) **471**, 83 (2011).

[31] Z. K. Fu, P. J. Wang, S. J. Chai, L. H. Huang, and J. Zhang, Phys. Rev. A **84**, 043609(2011).

[32] B. M. Anderson, J. M. Taylor, and V. M. Galitski, Phys. Rev. A **83**, 031602(R) (2011).

[33] F. Wilczek and A. Zee, Phys. Rev. Lett. **52**, 2111 (1984).

[34] We note that the setting of the velocity is appropriate since our system can also begin with a larger drifting velocity just as the same as the Raman interferometer.

[35] L. Alan, T. Hammond, E. Smith, M. Chapmen, R. Rubenstein and D. Pritchard, Phys. Rev. Lett. **78**, 760 (1997).